Dynamic modeling in large-eddy simulation of turbulent channel flow

Investigation of two-dimensional versus three-dimensional test filtering

Received April 2002
Revised August 2003
Accepted October 2003

Jessica Gullbrand
Center for Turbulence Research, Stanford University, Stanford, California, USA

Keywords *Simulation, Turbulent flow, Eddy currents, Tests and testing*

Abstract *Large-eddy simulation (LES) of a turbulent channel flow is performed using different subfilter-scale (SFS) models and test filter functions. The SFS models used are the dynamic Smagorinsky model (DSM) and the dynamic mixed model (DMM). The DMM is a linear combination between the scale-similarity model and the DSM. The test filter functions investigated are the sharp cut-off (in spectral space) and smooth filter that is commutative up to fourth-order. The filters are applied either in the homogeneous directions or in all three spatial directions. The governing equations are discretized using a fourth-order energy-conserving finite-difference scheme. The influence from the test filter function and the SFS model on the LES results are investigated and the effect of two-dimensional versus three-dimensional test filtering are investigated. The study shows that the combination of SFS model and filter function highly influences the computational results; even the effect on the zeroth-order moment is large.*

Introduction

In large-eddy simulation (LES), a low-pass filter is applied to the governing equations. This filtering procedure divides the flow field into resolved scale motions and subfilter-scale (SFS) motions. The SFS motions consist of scales that are damped by the filter function used and/or scales that are smaller than the smallest resolved length scale (Carati *et al.*, 2001; Gullbrand and Chow, 2003).

The most commonly used LES approach is the implicitly filtered approach. In implicitly filtered LES, the computational grid and the discretization operators are considered as the filtering of the governing equations. The advantage is that the procedure requires no implementation of filters. The drawback is that the filter function used cannot be determined, which can make SFS modeling more difficult.

The author wishes to thank Prof Oleg V. Vasliyev for providing the channel flow code and Prof Parviz Moin for his helpful discussions. He also thanks Fotini K. Chow for commenting on this paper.

International Journal of Numerical Methods for Heat & Fluid Flow
Vol. 14 No. 4, 2004
pp. 467-492

0961-5539
DOI 10.1108/09615530410532259

An alternative to implicitly filtered LES is to use explicit filtering. In the explicit approach, a filter function is chosen and applied in the simulations. Recently this approach has gained increased interest from the research community (Gullbrand, 2002; Gullbrand and Chow, 2003; Stolz *et al.*, 2001; Winckelmans *et al.*, 2001). The explicit filtering approach seems to be very promising as computer capacity is increasing, but further investigations are needed to make it applicable to flow fields of engineering interest.

In this paper, the implicitly filtered LES approach is used, since the study is aimed at investigating dynamic modeling for flow fields of engineering interest. The flow field investigated is the turbulent channel flow. The channel flow is a simplified turbulent flow field, but it serves as a good test case since it is well documented (Moser *et al.*, 1999) and has only one inhomogeneous direction. Traditionally, in channel flow simulations, the homogeneous directions of the flow field are used in the procedure for determining the contribution from the dynamic model. Flow fields of engineering interest usually involve complex geometries where there is no homogeneous direction. Therefore, an alternative procedure must be used where the three dimensionality of the flow field needs to be considered in the modeling procedure. This paper presents a detailed investigation of the effects of using a three-dimensional test filter in the dynamic procedure, as well as the effect of using the same filter as a local averaging of the dynamic coefficient to prevent numerical instability. The difficulty of creating a model for the resolved SFS motions in implicitly filtered LES is also addressed.

First, three-dimensional test filtering in the dynamic modeling of the SFS stresses is investigated. The influence of test filtering in the inhomogeneous direction is important to determine since, its effect also enters into the predicted results of more complex flow fields. The impact from three-dimensional test filtering is studied by comparing the results to those predicted by using two-dimensional filtering. To determine appropriate filter functions for filtering in inhomogeneous directions, special care is needed to avoid introducing commutation errors into the simulations (Ghosal, 1995; Ghosal and Moin, 1995). Therefore, a general theory for constructing discrete filters that commute up to desired order was developed by Vasilyev *et al.* (1998). To minimize the commutation error in the inhomogeneous direction, a filter function that is commutative to at least the same order as the numerical scheme used is needed. The effect of these high-order commutative filter functions on the LES results still needs to be determined. Earlier investigations on the influence of different filter functions on LES results focused on two-dimensional test filters which do not need to be commutative (Lund and Kaltenbach, 1995; Najjar and Tafti, 1996; Piomelli *et al.*, 1988; Sarghini *et al.*, 1999). A commutative test filter function is used in the simulations presented in this study to examine the effect of three-dimensional filtering without introducing commutation errors. Furthermore, the effect from the commutative

filters on the SFS stresses needs to be determined. This is investigated by performing a simulation applying a commonly used test filter function (the sharp cut-off filter) and comparing the results to those obtained using the commutative filter function.

Two dynamic SFS models are applied in this study: the dynamic Smagorinsky model (DSM) by Germano *et al.* (1991) and the dynamic mixed model (DMM). The DMM used here is a linear combination of the scale-similarity model (SSM) by Liu *et al.* (1994) and the DSM. In DSM, a test filter function is used to determine the dynamic coefficient, and the coefficient is traditionally averaged in the homogeneous directions of the channel flow. The test filter function commonly used is a sharp cut-off filter (in spectral space) in the homogeneous directions. Since a sharp cut-off filter is difficult to apply in more general flow cases, the influence of using a smooth test filter needs to be determined. Furthermore, the test filter function chosen is a reflection of the assumption of the implicit filter function. The dynamic procedure is based upon a similarity assumption which requires the test filter function to be similar to the implicit filter (Carati and Eijnden, 1997). The difficulty with the implicitly filtered LES approach is that the shape of the implicit filter function is unknown and therefore, an appropriate test filter function cannot be chosen. In the explicitly filtered LES approach, the filter function applied to the governing equations is known and the resolved SFS part can therefore be reconstructed (Gullbrand and Chow, 2003). This is not applicable in implicitly filtered LES and therefore a model is needed for the resolved SFS part. Note that an SFS model for the resolved stresses is only valid when assuming the implicit filter function to be a smooth filter function. When applying a sharp cut-off filter, all the motions that are larger than the cut-off length-scale are assumed to be resolved. In this paper, the SSM by Liu *et al.* (1994) is used as a first approximation of an appropriate SFS model for the resolved SFS part.

Finally, the effect of the averaging procedure applied to the dynamic model coefficient is evaluated. In DSM, the model coefficient is calculated dynamically during the entire simulation. However, the coefficient value may vary rapidly in the computational domain leading to numerical instability. To avoid this problem, Germano *et al.* (1991) suggested averaging the model coefficient in the homogeneous directions of the channel flow. This averaging procedure may not be feasible in flow fields of engineering interest and the coefficient may need to be averaged locally. Ghosal *et al.* (1995) proposed a dynamic localization model to avoid the problem. However, this is a rather complicated method, which involves solving an additional integral equation. Therefore, in the investigation presented, a simple approach is examined where the dynamic coefficient is averaged locally with the test filter function used. It is an easy approach which does not require implementation of any additional filter function or procedure. This averaging procedure was earlier proposed by

Zang *et al.* (1993), and applied to a recirculating flow field. However, the influence on the LES results from the locally averaged and homogeneously averaged model coefficient need to be determined.

The simulations presented in this paper are performed with a fourth-order finite-difference scheme in addition to using a fourth-order commutative filter function. The SFS models typically use information from the smallest resolved length scales to model the SFS contribution. It is therefore of great importance, that these resolved length scales are captured accurately. This requires that the numerical error of the scheme be sufficiently small and thereby the use of high-order discretization and a high-order commutative filter function. All the LES results are compared to DNS data by Moser *et al.* (1999).

Governing equations

In LES, the governing equations are filtered in space. The low-pass filter function G is applied to the flow variable f

$$\bar{f}(x, \Delta, t) = \int_{-\infty}^{\infty} G(x, x', \Delta) f(x', t)\, \mathrm{d}x' \tag{1}$$

where Δ is the filter width.

The governing equations for incompressible flows are the filtered continuity equation and the Navier-Stokes, written as

$$\frac{\partial \bar{u}_i}{\partial x_i} = 0 \tag{2}$$

$$\frac{\partial \bar{u}_i}{\partial t} + \frac{\partial \bar{u}_i \bar{u}_j}{\partial x_j} = -\frac{\partial \bar{p}}{\partial x_i} + \frac{1}{\mathrm{Re}_\tau} \frac{\partial^2 \bar{u}_i}{\partial x_j^2} - \frac{\partial \tau_{ij}}{\partial x_j} \tag{3}$$

where u_i denotes velocity vector, p pressure, and Re_τ the Reynolds number based upon the friction velocity and channel half-width. τ_{ij} is the SFS stress tensor defined as $\tau_{ij} = \overline{u_i u_j} - \bar{u}_i \bar{u}_j$.

The SFS stress tensor includes the turbulence motions from scales that are damped by the filter function and/or scales that are smaller than the grid size resolution (Carati *et al.*, 2001). In implicitly filtered LES, both damped turbulence motions and unresolved motions need to be modeled. This is done with SFS models.

Subfilter-scale models

Since implicitly filtered LES are used in the simulations presented, both resolved and unresolved SFS stresses need to be modeled. On the other hand, in explicitly filtered LES, the resolved SFS stresses can be reconstructed by an inverse filtering procedure. Different approximations in the inverse filtering

procedure have been proposed in the literature (Chow and Street, 2002; Stolz *et al.*, 2001), and one of the models that can be obtained from this procedure is the SSM by Bardina *et al.* (1980). In the explicit filtering approach, even though a model is used for the resolved SFS stresses, the unresolved SFS stresses must still be modeled. The unresolved SFS stresses contain motions that are smaller than the smallest resolved length scale. This term is usually denoted as the sub-grid scale (SGS) stresses. Note that the SSM by Bardina *et al.* (1980) requires the use of explicit filtering.

The SSM by Liu *et al.* (1994) is used in these simulations as the model for the resolved SFS stresses, while the DSM is used for the unresolved stresses. Since an SFS model cannot be reconstructed for the resolved stresses, the SSM by Liu *et al.* (1994) is chosen as it is similar to the model by Bardina *et al.* (1980). Both models are based upon a similarity assumption, but the model by Liu *et al.* (1994) uses information from length scales larger than in the model by Bardina *et al.* (1980). The SSM by Liu *et al.* is written as $\left(\widehat{\bar{u}_i\bar{u}_j} - \widehat{\bar{u}}_i\widehat{\bar{u}}_j\right)$, where the tophat symbol ($\widehat{\ }$) denotes filtering with a test filter function with larger filter width than the implicit filter. The total expression for the SFS stresses with both scale-similarity term and DSM is

$$\tau_{ij} = \widehat{\bar{u}_i\bar{u}_j} - \widehat{\bar{u}}_i\widehat{\bar{u}}_j - 2(C_s\Delta)^2|\bar{S}|\bar{S}_{ij},$$

where C_s is the dynamic model coefficient in the DSM and S_{ij}, is the strain rate tensor. A coefficient could be placed in front of the scale-similarity term, however this is not investigated in this work and is left for future studies.

The dynamic procedure in the DSM uses the same test filter function as in the SSM by Liu *et al.* (1994) to determine the model coefficient. In the simulations, it is the $(C_s\Delta)^2$ term that is calculated dynamically. The advantage of solving for $(C_s\Delta)^2$ instead of only C_s is to avoid the ambiguity in determining the filter width used in the DSM when stretched meshes are used (Scotti *et al.*, 1996). When solving for $(C_s\Delta)^2$, it is only the ratio between the test filter width and the implicit filter that is employed. The least-square approximation by Lilly (1992) is used to solve the six independent equations to obtain one model coefficient. To simplify the notation used in this paper, the $(C_s\Delta)^2$ term is hereafter denoted as C.

To avoid numerical instabilities, the dynamic model coefficient is usually averaged in the homogeneous directions of the channel flow (Germano *et al.*, 1991). This averaging procedure, denoted with $\langle C\rangle$, is compared to a locally averaged procedure. The local averaging is performed by filtering the coefficient using the test filter function ($\hat{C}$). This local averaging was earlier used by Zang *et al.* (1993), but they used another test filter function in their simulations. The local averaging of the coefficient is of interest when more complex flow fields are considered, and to the authors knowledge there has been no comparisons between the two methods in order to determine the impact on the LES results from each averaging procedure.

In the simulations, the total eddy viscosity is clipped, if the value from the DSM is largely negative. The criteria used is the same as applied by Zang *et al.* (1993) that prevents the total eddy viscosity from becoming negative:

$$\nu_{\text{total}} \leq \nu_{\text{DSM}} + \nu_{\text{molecular}}$$

Filters

Two test filters, i.e. one fourth-order commutative filter function and one sharp cut-off filter, are used in the simulations. The simulations are performed using a fourth-order finite-difference scheme and therefore, in order to minimize the commutation error, a filter function that is at least commutative up to fourth-order is needed. In the channel flow case, it is only in the inhomogeneous direction of the flow that a commutation error might be introduced. The fourth-order commutative filter was developed using the theory proposed by Vasilyev *et al.* (1998).

The two test filter functions are shown in spectral space in Figure 1. In physical space, the discrete fourth-order commutative filter is

$$\hat{\phi}_i = -\frac{1}{32}\phi_{i-3} + \frac{9}{32}\phi_{i-1} + \frac{1}{2}\phi_i + \frac{9}{32}\phi_{i+1} - \frac{1}{32}\phi_{i+3}, \tag{5}$$

where the filter weights for $\phi_{i\pm2}$ are zero.

In the simulations, the filter functions are employed only when calculating the SFS contribution. A test filter is used in the dynamic procedure of the DSM and when determining the contribution from the SSM part (Liu *et al.*, 1994). The commutative filter function is used both in two-dimensional test filter cases and three-dimensional ones. The sharp cut-off filter is used only in the two-dimensional filter studies. Note that when using the sharp cut-off filter in the DMM, the contribution from the SSM vanishes and only the contribution

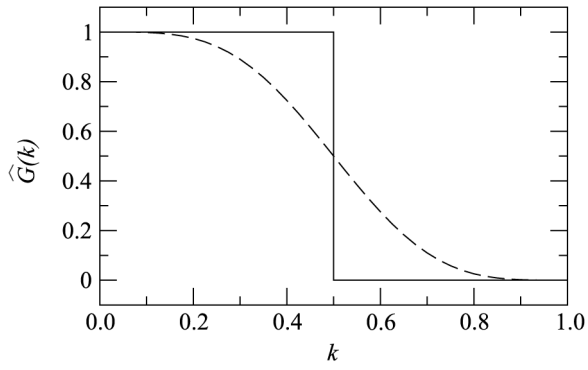

Note: —— : Sharp cutoff filter, and — — — : fourth-order commutative filter

Figure 1.
Filter function $\hat{G}(k)$ as a function of the wavenumber k

from the DSM remains. Therefore, the DMM is not used with the sharp cut-off filter.

The ratio between the test filter width and the computational cell size is chosen to be $\Delta_{\text{test}}/\Delta_{\text{grid}} = 2$. This is the value that was recommended by Germano *et al.* (1991) for the test filter width in the DSM. For the fourth-order commutative filter function, the filter width is determined by where $\hat{G}(k) = 0.5$ and as seen in Figure 1, $k\Delta/\pi = 0.5$ at this location. This corresponds to an effective filter width of 2Δ (Lund, 1997).

Solution algorithm

The space derivatives in the governing equations are discretized using a fourth-order finite-difference scheme on a staggered grid. The convective terms are discretized in a skew-symmetric form to ensure conservation of turbulent kinetic energy (Morinishi *et al.*, 1998; Vasilyev, 2000). The equations are integrated in time with the third-order Runge-Kutta scheme described by Spalart *et al.* (1991). The diffusion terms in the wall-normal direction are treated implicitly with the Crank-Nicolson scheme to ease the constraint on the time step of the scheme. The splitting method of Dukowicz and Dvinsky (1992) is used to enforce the solenoidal condition. The resulting discrete Poisson equation of pressure is solved using a penta-diagonal direct matrix solver in the wall-normal direction and a discrete Fourier transform in the homogeneous/periodic directions. Periodic boundary conditions are applied in the streamwise and spanwise directions, while no slip conditions are applied at the walls. A fixed mean pressure gradient is used in the streamwise direction. An evaluation of the fourth-order energy-conserving scheme and a comparison with a second-order conservative scheme are reported by Gullbrand (2000) and Gullbrand and Chow (2003).

Turbulent channel flow simulations

The Reynolds number of the turbulent channel flow is $\text{Re}_\tau = 395$ and the computational domain is ($2\pi h$, $2h$, πh) in the streamwise (x), wall-normal (y) and spanwise (z) directions, respectively. A computational grid resolution of (36, 37, 36) is used. The grid is stretched in the wall-normal (j) direction according to

$$y(j) = \frac{\tanh\left(\gamma\left(\frac{2j}{N_2} - 1\right)\right)}{\tanh(\gamma)}, \quad j = 0, \ldots, N_2 \tag{6}$$

where N_2 is the number of grid points in the j-direction and γ is the stretching parameter. In the simulations, $\gamma = 2.75$ is used. The grid resolution corresponds to $\Delta x^+ = 69$, $0.5 \leq \Delta y^+ \leq 56$ and $\Delta z^+ = 34$ when normalized with the friction velocity and the kinematic viscosity. This resolution is very coarse and is near the limit of where LES is expected to perform well. However,

the coarse resolution is chosen because of the additional challenge it brings to the SFS models. As the resolution decreases, an increased emphasis is put on the models as an increasing portion of the energy spectrum is not resolved and therefore has to be modeled. In flow fields of engineering interest, fine resolution is often not feasible due to the complexity of the flow and the long computational times associated with LES. By using a coarse computational grid, larger emphasis is also put on the numerical scheme. A statistically stationary solution is obtained after 60 dimensionless time units and thereafter, statistics are sampled during 30 time units. The time is normalized by the friction velocity and the channel half-width. The statistics are compared to the unfiltered DNS data of Moser *et al.* (1999). The LES results are averaged in time and in the homogeneous direction if not stated otherwise.

In order to verify that the results presented in this study is not an artifact of too coarse grid resolution, the same simulations were performed using a resolution of (64, 49, 48). This resolution is a quarter of the DNS resolution in each spatial direction. The same trends were observed in the LES results for both resolutions; (36, 37, 36) and (64, 49, 48). However, the differences in the results predicted by the different models were smaller on the finer grid resolution. As the resolution increases more length scales are resolved and therefore, less influence is expected from the models on the LES results.

Results

The LES results predicted by the DSM and the DMM are presented in this section. The test filtering is performed in two or three dimensions. The sharp cut-off filter is used only for the two-dimensional test filtering, while the fourth-order commutative filter function is applied in both two and three dimensions. The LES results are compared to DNS data for mean velocity profiles and reduced (deviatoric) turbulence intensities. Note that these turbulence intensities are adjusted by removing the trace from each tensor component, as discussed by Winckelmans *et al.* (2002). The values predicted by the SFS models are compared between the different simulations for the dynamic model coefficient, eddy viscosity, and modeled shear stress.

Two-dimensional test filtering

In this section, the test filter is applied only in the homogeneous directions (x, z). Both sharp cut-off filter and fourth-order commutative filter have been used to calculate the contribution from the SFS models.

The DSM versus the DMM. As seen in Figure 2, the mean velocity profiles predicted by the DSM with the sharp cut-off test filter and the DMM (commutative test filter) are relatively close to the the DNS data. The mean velocities predicted by the LES all over-predict the velocity in the log-law region. The difference between the DMM and the DSM with the sharp cut-off

filter is small. The largest over-prediction is predicted by the DSM with the commutative filter.

While the DSM with the sharp cut-off filter predicts the best velocity profile, the reduced turbulence intensities predicted by the DMM are closer to the DNS data (Figure 3). The absolute value of the intensities predicted by the LES are

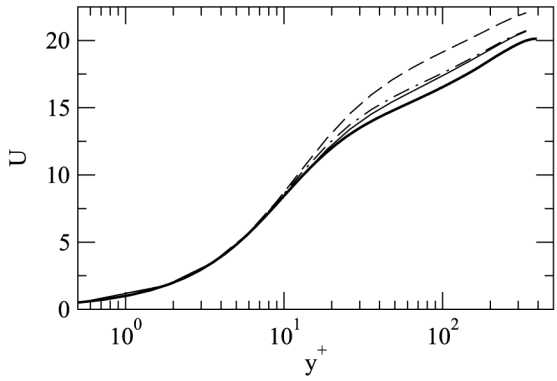

Note: —— : DNS data, —— : DSM using sharp cutoff filter, — — — : DSM using fourth-order commutative filter and · — · — : DMM using fourth-order commutative filter

Figure 2.
Mean velocity profiles using two-dimensional test filtering and grid resolution (36, 37, 36)

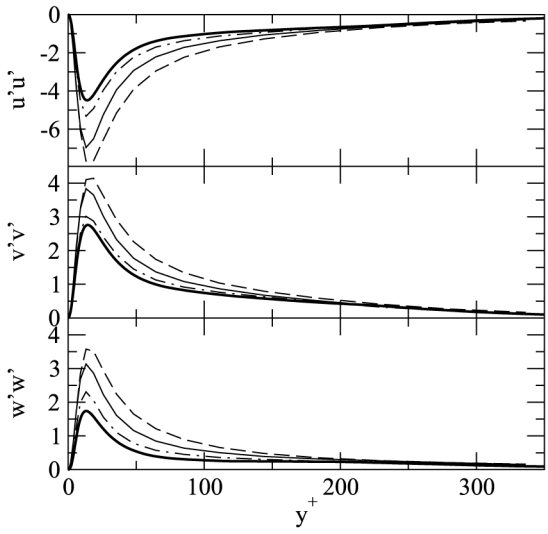

Note: —— : DNS data, —— : DSM using sharp cutoff filter, — — — : DSM using fourth-order commutative filter and · — · — : DMM using fourth-order commutative filter

Figure 3.
Reduced turbulence intensities in streamwise $u'u'$, wall-normal $v'v'$, and spanwise $w'w'$ directions using two-dimensional test filtering and grid resolution (36, 37, 36)

all larger than the DNS results. As shown for the mean velocity profiles, the worst results are predicted by the DSM when used with the commutative filter function.

Figure 4 shows the dynamic model coefficient predicted by the DSM. The value of the coefficient increases as the test filter function changes from the sharp cut-off filter to the commutative filter. Using the commutative test filter, the DSM predicts smaller coefficient values when used in combination with the SSM. The same trend as observed for $\langle C \rangle$ is also seen for the eddy viscosity, $\nu_{\mathrm{DSM}} = C|\bar{S}|$ (Figure 5). This indicates that the absolute value of the strain rate

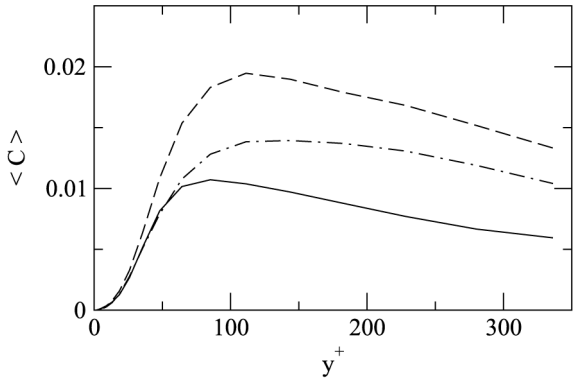

Note: —— : DSM using sharp cutoff filter, — — — : DSM using fourth-order commutative filter and · — · — : DMM using fourth-order commutative filter

Figure 4.
Model parameter $\langle C \rangle$ predicted by the DSM using two-dimensional test filtering and grid resolution (36, 37, 36)

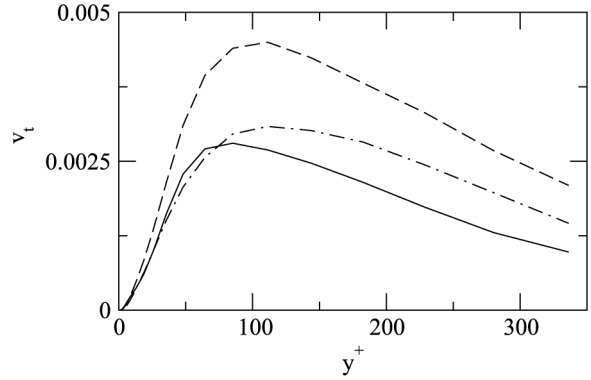

Note: —— : DSM using sharp cutoff filter, — — — : DSM using fourth-order commutative filter and · — · — : DMM using fourth-order commutative filter

Figure 5.
Eddy viscosity ν_t predicted by the DSM using two-dimensional test filtering and grid resolution (36, 37, 36)

is not very different in the simulations. Therefore, the increased eddy viscosity predicted by the DSM when used with the commutative test filter seems to be mainly an effect of the increased value of the model coefficient.

Figure 6 shows the modeled shear stress τ_{12}, where index 1 denotes the x-direction and 2 the y-direction. The DMM predicts the largest modeled shear stress and the SSM portion of the model contributes with the largest stress. Actually, the SSM stress is more than twice as large as the DSM contribution. When the DSM is used alone, the predicted shear stress increases, when used with the commutative test filter compared to the sharp cut-off filter.

The results presented in this section, indicate that the increased over-prediction of the mean velocity profile and reduced turbulence intensities predicted by the DSM are a result of the increased value of the dynamic model coefficient. The model coefficient increases when the test filter is smooth compared to when the sharp cut-off filter is used. The SSM seems to be a relatively good model of the resolved SFS stresses in the DMM. When studying the turbulence intensities, the DMM even predicts results better than the DSM when used with the sharp cut-off filter, despite the fact that the DSM with the sharp cut-off filter is a model that is known to predict good results in the channel flow simulations.

The DSM: homogeneous averaging versus local averaging. In this section, the concept of averaging the model coefficient in the DSM in either the homogeneous directions or locally (by using the test filter function) is studied. When averaging in the homogeneous directions, the computational data in the whole plane (streamwise and spanwise directions) are used. By using the test filter, only the closest computational grid points are used in the averaging procedure. The stencil of the filter function determines the number of grid

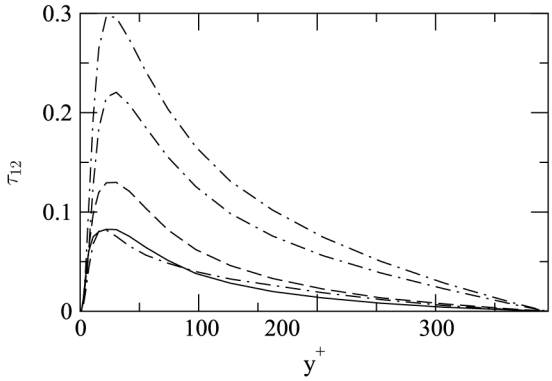

Note: ——— : DSM using sharp cutoff filter, – – – : DSM using fourth-order commutative filter and ·—·—· : DMM using fourth-order commutative filter. Lower curve: DSM contribution, middle curve: SSM contribution, and upper curve: total contribution

Figure 6.
Modeled shear stress τ_{12} using two-dimensional test filtering and grid resolution (36, 37, 36)

points that are involved in the averaging. Therefore, the test filter function results in a local averaging of the model coefficient. The term local averaging is used to describe the model coefficient averaged with the test filter function. The study is performed for the DSM when used with the commutative filter function only.

The comparison of the mean velocity profiles for the two different averaging procedures is shown in Figure 7. The mean velocity profile in the log-law region improves significantly when the local averaging of the model coefficient is applied. The results from using the local averaging are comparable to the ones predicted using the sharp cut-off filter shown in Figure 2.

The reduced turbulence intensities are also improved when local averaging is used compared to the homogeneous averaging (Figure 8). The peak value of the turbulence intensities when using local averaging are comparable to the DMM results in Figure 3, and both DSM local averaging and DMM are close to the DNS predictions. However, the peaks of the turbulence intensities are broader for the DSM with local averaging than for the DMM results.

An instantaneous spanwise profile of the model coefficient C in the DSM is shown in Figure 9. The data is calculated *a priori* from an instantaneous flow field where no SFS models have been used. Large fluctuations in the value of the model coefficient and large negative values may result in numerical instabilities. Therefore, it is of interest to reduce the peaks or smooth them out. The two procedures investigated here are filtering the coefficient using the test filter function or averaging the coefficient in the homogeneous directions. The results from both procedures is seen in Figure 9. In the simulations, small negative values are allowed while large negative values are clipped.

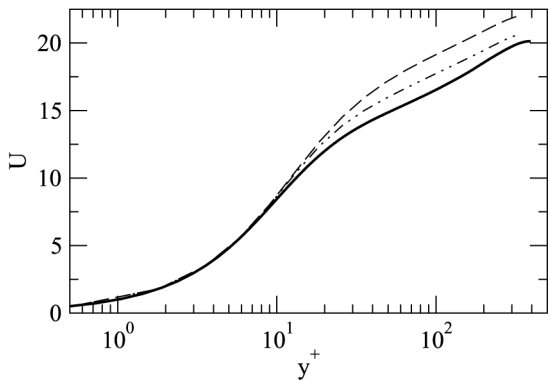

Note: ——— : DNS data, – – – : DSM using fourth-order commutative filter and homogenous averaging, and ·–·–· : DSM using fourth-order commutative filter and local averaging

Figure 7.
Mean velocity profiles using two-dimensional test filtering and grid resolution (36, 37, 36)

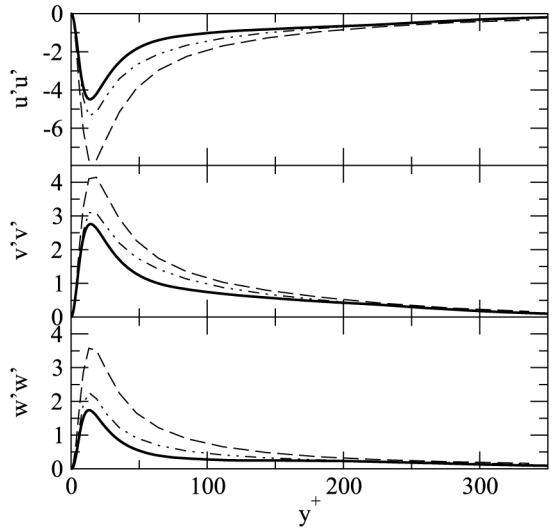

Note: ——— : DNS data, – – – : DSM using fourth-order commutative filter and homogenous averaging, and – · – · – : DSM using fourth-order commutative filter and local averaging

Figure 8.
Reduced turbulence intensities in streamwise $u'u'$, wall-normal $v'v'$ and spanwise $w'w'$ directions using two-dimensional test filtering and grid resolution (36, 37, 36)

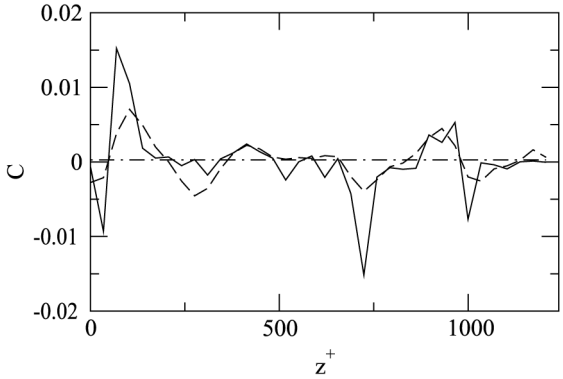

Note: ——— : C: DSM data using fourth-order commutative filter before averaging, – – – : $\widehat{C}$: DSM data using fourth-order commutative filter and local averaging, and – · – · – : $< \widehat{C} >$: DSM data using fourth-order commutative filter and homogeneous averaging ($< \widehat{C} >$=0.00028)

Figure 9.
Model parameter C in the DSM calculated from an instantaneous flow field in the center of the domain using two-dimensional test filtering and grid resolution (36, 37, 36)

The clipping value is chosen to be $-1/\mathrm{Re}_\tau$, in order to avoid negative dissipation in the momentum equations.

Variations of locally averaged model coefficient is shown in a horizontal cross-section in Figure 10. Regions of positive and negative values of the model coefficient are observed.

The value of the predicted eddy viscosity is larger when using local averaging (Figure 11). In the center part of the channel flow ($y^+ > 100$), an almost constant relation is observed between the two eddy viscosities, however, the curves deviate from each other close to the wall.

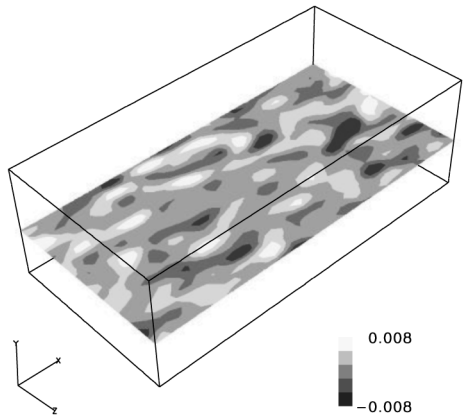

Note: Black contour represents negative values and white positive ones

Figure 10.
Model parameter C in the DSM in the center plane of the domain calculated from an instantaneous flow field using two-dimensional test filtering and grid resolution (36, 37, 36)

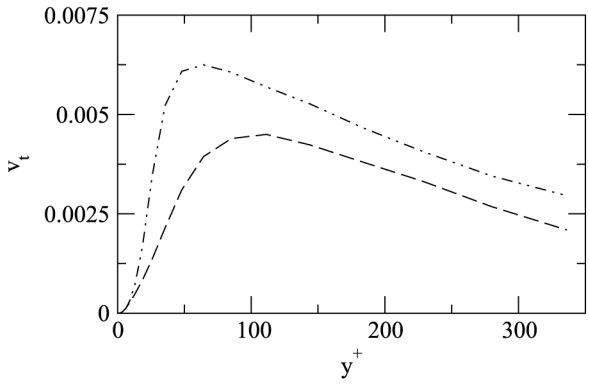

Note: − − − : DSM using fourth-order commutative filter and homogenous averaging, and ·−·−· : DSM using fourth-order commutative filter and local averaging

Figure 11.
Eddy viscosity ν_t from the DSM using two-dimensional test filtering and grid resolution (36, 37, 36)

Figure 12 shows a larger peak value of the modeled SFS shear stress when local averaging is used compared to the homogeneously averaged one. Otherwise, the shape of the curves are very similar.

By allowing the model coefficient to fluctuate in the plane, the locally averaged DSM predicts the mean velocity profile and peak values of turbulence intensities that are very similar to what is predicted by the DMM. Larger local fluctuations are introduced by the local averaging that seem to be comparable to the DMM results, even though the modeled shear stresses are very different between the two simulations.

Three-dimensional filtering

In this section, three-dimensional test filtering using a fourth-order commutative filter function is applied when calculating the SFS stresses.

The DSM versus the DMM. As shown in Figure 13, the DSM with the three-dimensional test filtering over-predicts the mean velocity profile in the log-law region, while the DMM is unable to capture the log-law behavior in the center of the channel. The mean velocity profile predicted by the DMM starts to deviate from the log-law just below $y^+ = 100$. This is due to the three-dimensional filtering of the SSM, indicating that the resolution in the wall-normal direction is too coarse in the center of the channel for the SSM. When the grid resolution is doubled in the wall-normal direction, the results are improved greatly. The results are also improved if the coarse grid resolution is used and the test filtering of the SSM is performed only in the two homogeneous directions. Using the finer grid resolution in the wall-normal direction or the two-dimensional filtering of the SSM, the mean velocity profile is very close to the DNS results. Since the LES results are expected to improve,

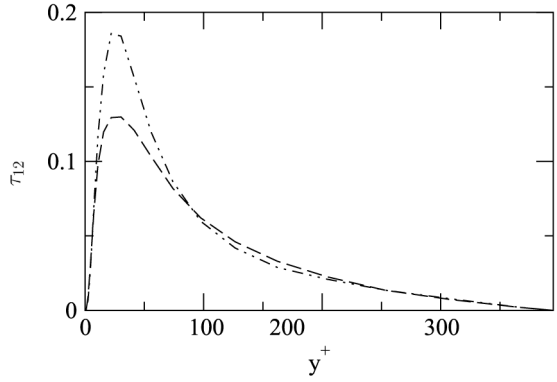

Note: – – – : DSM using fourth-order commutative filter and homogenous averaging, and – · · · – · : DSM using fourth-order commutative filter and local averaging

Figure 12.
Modeled shear stress τ_{12} using two-dimensional test filtering and grid resolution (36, 37, 36)

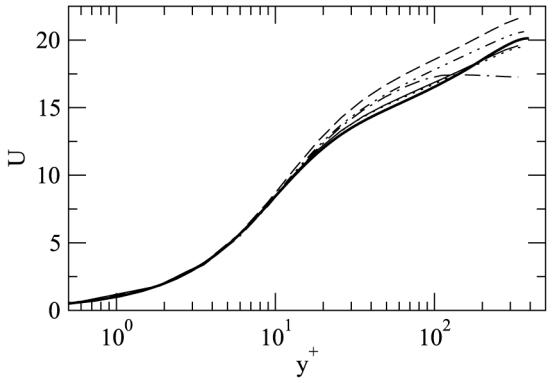

Note: ——— : DNS data, ——— : DMM using fourth-order commutative two-dimensional filtering of SSM and three-dimensional filtering of DSM and grid resolution (36,37,36), ····· : DMM using fourth-order commutative filter and grid resolution (36,73,36), – – – : DSM using fourth-order commutative filter and grid resolution (36,37,36), · — · — · : DMM using fourth-order commutative filter and grid resolution (36,37,36), and · – · · – · : DSM using fourth-order commutative filter and grid resolution (36,73,36)

Figure 13.
Mean velocity profiles using three-dimensional test filtering

as the resolution is refined, the DSM with the finer grid resolution in the wall-normal direction is performed for comparison purposes. The DSM using the finer grid predicts a mean velocity profile that is similar to the DMM on the coarser grid in the near wall region. The DSM shows no difficulties in capturing the log-law region for either grid resolution. However, for the finer grid resolution the mean velocity profile predicted by the DMM is closer to the DNS data than the DSM results.

The peak values of the turbulence intensities are fairly well captured by the DMM (Figure 14), even though the DMM breaks down in the center of the channel. The turbulence intensities predicted by the DMM show a small bump after $y^+ = 100$, for all intensities. The bump is clearly seen in the predicted spanwise intensity. As for the DSM, the turbulence intensities in all three directions are very similar to the ones predicted using two-dimensional test filtering. The intensities predicted when using the DMM with the finer wall-normal resolution or the DMM using the coarse grid and two-dimensional test filtering of the SSM, both show good agreement with the DNS data. The DSM with the fine wall-normal resolution does not show large improvements in the turbulence intensities predicted. Therefore for the DSM, large over-prediction of the intensities seems to depend upon the resolution in the homogeneous directions to a larger degree, than the wall-normal resolution.

The value of the dynamic model coefficient is smaller when used in the DMM as shown in Figure 15. The same observation was made for the coefficient when two-dimensional test filtering was applied. However, the model

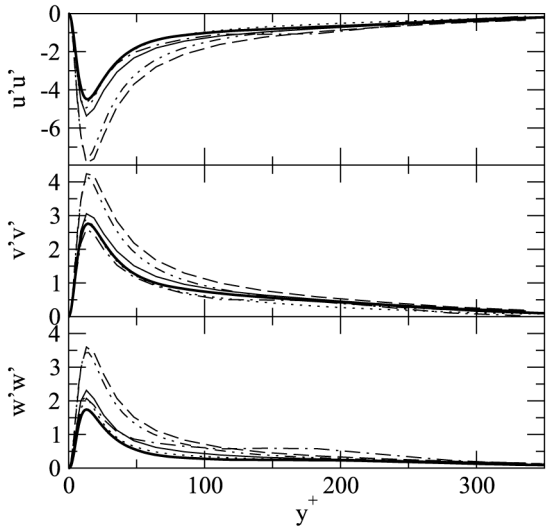

Note: ——— : DNS data, ——— : DMM using fourth-order commutative two-dimensional filtering of SSM and three-dimensional filtering of DSM and grid resolution (36,37,36), ····· : DMM using fourth-order commutative filter and grid resolution (36,73,36), – – – : DSM using fourth-order commutative filter and grid resolution (36,37,36), – · – · : DMM using fourth-order commutative filter and grid resolution (36,37,36), and – ·· – · : DSM using fourth-order commutative filter with grid resolution (36,73,36)

Figure 14.
Reduced turbulence intensities in streamwise $u'u'$, wall-normal $v'v'$ and spanwise $w'w'$ directions using three-dimensional test filtering

coefficient for the DMM when using the coarse grid and three-dimensional filtering shows a rather strange behavior. The value of the coefficient becomes negative on an average. When the resolution is increased or two-dimensional filtering of the SSM is applied, the shape of the curves for the model coefficient are closer to those previously seen in Figure 4. By increasing the wall-normal resolution, the value of the model coefficient is decreased in the center of the channel and its predicted peak value is closer to the wall. Even though the value of the model coefficient is very similar in the two cases (increased grid resolution or filtering of the SSM in two dimensions), the finer resolution results in a smaller eddy viscosity (Figure 16). This is due to the fact that the finer grid resolution resolves more length scales and therefore, the effect from the SFS model is reduced. The same behavior is observed for the DSM as the grid resolution is increased in the wall-normal direction. The eddy viscosity predicted by the DMM shows the same peculiar behavior as observed for the model coefficient on the coarse resolution. The largest eddy viscosity is predicted by the DSM.

The largest contribution to the modeled shear stress is predicted by the DMM where the SSM part is considerably larger than the DSM portion as

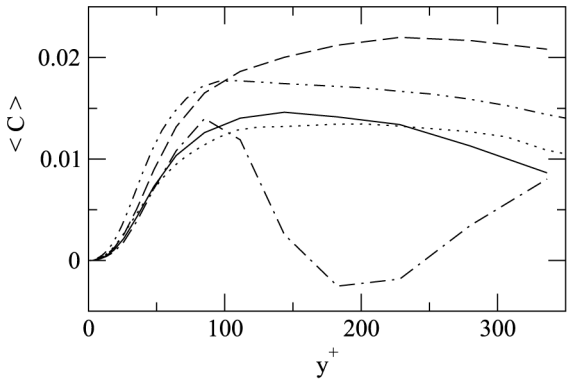

Note: ——— : DMM using fourth-order commutative two-dimensional filtering of SSM and three-dimensional filtering of DSM and grid resolution (36,37,36), ····· : DMM using fourth-order commutative filter and grid resolution (36,73,36), — — — : DSM using fourth-order commutative filter and grid resolution (36,37,36), — · — · : DMM using fourth-order commutative filter and grid resolution (36,37,36), and — · — · : DSM using fourth-order commutative filter with grid resolution (36,73,36)

Figure 15.
Model parameter ⟨*C*⟩ from the DSM using three-dimensional test filtering

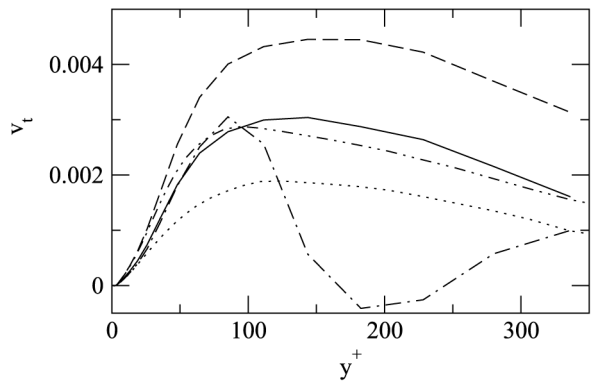

Note: ——— : DMM using fourth-order commutative two-dimensional filtering of SSM and three-dimensional filtering of DSM and grid resolution (36,37,36), ····· : DMM using fourth-order commutative filter with grid resolution (36,73,36), — — — : DSM using fourth-order commutative filter and grid resolution (36,37,36), — · — · : DMM using fourth-order commutative filter and grid resolution (36,37,36), and — · — · : DSM using fourth-order commutative filter with grid resolution (36,73,36)

Figure 16.
Eddy viscosity contribution from the DSM using three-dimensional test filtering

shown in Figure 17. The figure explains the strange behavior of the model coefficient and the eddy viscosity, Figures 15 and 16, respectively, in the DMM for the coarse resolution and three-dimensional test filtering. The SSM predicts too large shear stress in the center of the flow field (above $y^+ = 100$). The shear stress predicted by the DSM rapidly decreases to reduce the total influence from the DMM. However, the reduction in the DSM is not enough to counteract the influence from the SSM. The eddy viscosity predicted is prevented from becoming largely negative because of the clipping procedure to avoid negative total viscosity. Therefore, the DSM is not able to fully counteract the behavior of the SSM or have a larger influence on the results. For the DSM used alone, the fine grid resolution in the wall-normal direction results in a smaller shear stress predicted.

The DSM: homogeneous averaging versus local averaging. Local averaging in three dimensions of the model coefficient in the DSM reduces the over-prediction of the mean velocity profile compared to homogeneous averaging (Figure 18). The same trend was observed in the results for the two-dimensional test filtering. However, for the three-dimensional test filtering, the relative improvement of the velocity profile when using local averaging is smaller, because the results of the DSM using homogeneous averaging are improved initially when three-dimensional test filtering is applied. The mean velocity profiles predicted using local averaging show very small dependence upon two-dimensional or three-dimensional test filtering (compare Figures 7 and 18).

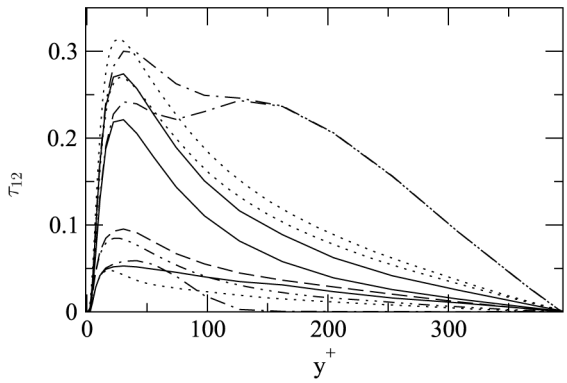

Note: —— : DMM using fourth-order commutative two-dimensional filtering of SSM and three-dimensional filtering of DSM and grid resolution (36,37,36), ····· : DMM using fourth-order commutative filter and grid resolution (36,73,36), — — — : DSM using fourth-order commutative filter and grid resolution (36,37,36), — · — · : DMM using fourth-order commutative filter and grid resolution (36,37,36), and — · · — · · : DSM using fourth-order commutative filter with grid resolution (36,73,36)

Figure 17.
Modeled shear stress τ_{12} using three-dimensional test filtering

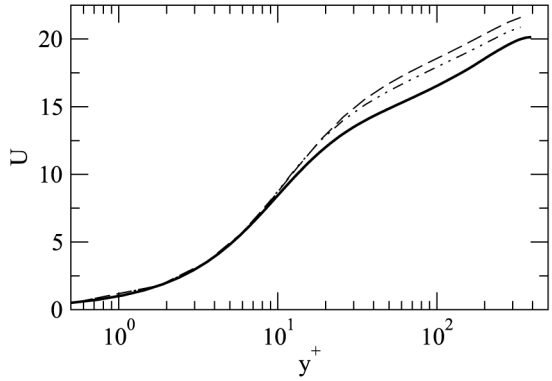

Note: ——— : DNS data, – – – : DSM using fourth-order commutative filter and homogeneous averaging, and – · · · – · : DSM using fourth-order commutative filter and local averaging

Figure 18.
Mean velocity profiles using three-dimensional test filtering and grid resolution (36, 37, 36)

The turbulence intensities are improved when using three-dimensional local averaging of the model coefficient in the DSM, (Figure 19). However, the turbulence intensities predicted by local averaging and test filtering in two dimensions (Figure 8) are closer to the DNS data than the results predicted by using three-dimensional test filtering. The peak values are higher and are

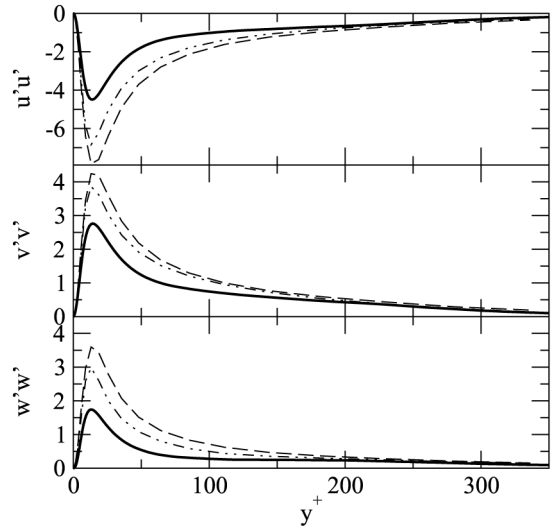

Note: ——— : DNS data, – – – : DSM using fourth-order commutative filter and homogeneous averaging, and – · · · – · : DSM using fourth-order commutative filter and local averaging

Figure 19.
Reduced turbulence intensities in streamwise $u'u'$, wall-normal $v'v'$ and spanwise $w'w'$ directions using three-dimensional test filtering and grid resolution (36, 37, 36)

broader when using local averaging and three-dimensional test filtering compared to the two-dimensional test filtered results. The turbulence intensities predicted by the DSM using homogeneous averaging of the model parameter are almost identical when test filtering is performed in either two dimensions or three dimensions.

The eddy viscosity predicted when using local averaging shows a sharper gradient in the near wall region (Figure 20). Otherwise, the maximum value of the eddy viscosity is not very different in the two simulations. The eddy viscosity predicted by the local averaging and two-dimensional test filtering is larger than the homogeneously averaged results (Figure 11), but this is not observed in the results when using three-dimensional test filtering. However, when the three-dimensional test filtering and local averaging are applied, the eddy viscosity fluctuates in the near wall region. This behavior was not observed for the two-dimensional filtering. The eddy viscosity increases in the first three grid points from the wall while lower viscosity is calculated in the next two points. In the first three grid points in the wall-normal direction, asymmetric commutative filter functions are used. A symmetric filter (equation (5)) is used in the rest of the flow field. The jump in the eddy viscosity corresponds to the change from the asymmetric filters to the symmetric one. This dependence is not observed when homogeneous averaging of the model parameter is used. However, the change from asymmetric to symmetric filter does not influence the computed results. A simulation was performed where the eddy viscosity was set to zero in the first three grid points. No effect was seen in the presented results. As long as the grid resolution is fine enough in the near wall region, the filters used there do not influence the results.

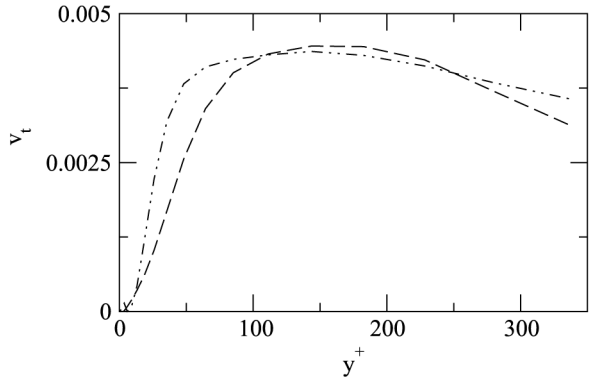

Note: – – – : DSM using fourth-order commutative filter and homogeneous averaging, and – · · · – : DSM using fourth-order commutative filter and local averaging

Figure 20.
Eddy viscosity ν_t contribution from the DSM using three-dimensional test filtering and grid resolution (36, 37, 36)

The peak value of the SFS shear stress is larger when local averaging is used (Figure 21). The near wall behavior observed in Figure 20 is also seen in the predicted shear stresses. For the shear stress, the same trend is observed for three-dimensional test filtering as for the two-dimensional one, that the peak value of the stresses predicted are larger when local averaging is used compared to the homogeneously averaged case. However, the values of the stresses are lower in the three-dimensional local averaging case when compared to the results using two-dimensional test filtering.

Discussion and conclusions

An investigation has been performed using dynamic modeling in LES using two- and three-dimensional test filtering in turbulent channel flow. The results of this study are intended for application to flow fields of engineering interest where it is of great importance to determine the influence of three-dimensional test filtering on the predicted LES results. The LES approach used is the implicitly filtered procedure, which is the most commonly used approach. In implicitly filtered LES, the computational grid and the discretization operators are considered to be the filtering of the governing equations. The test filtering is employed only in the dynamic modeling of the SFS stresses. Most test filtering in channel flow simulations has been performed only in the homogeneous directions, which is not applicable to complex geometries. In order to minimize the commutation error from test filtering in the inhomogeneous direction, a fourth-order commutative filter function is used. The commutative filter is a smooth filter function. A sharp cut-off filter is used in the investigation for comparison purposes. The implicit filter used in the simulations cannot be determined and the test filter function employed reflects the assumption of the shape of the implicit filter.

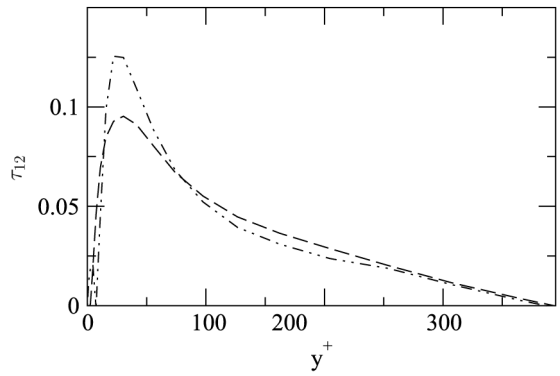

Note: – – – : DSM using fourth-order commutative filter and homogeneous averaging, and – · · · – · : DSM using fourth-order commutative filter and local averaging

Figure 21.
SGS shear stress τ_{12} from the DSM using three-dimensional test filtering and grid resolution (36, 37, 36)

The dynamic SFS models used in the simulations are the DSM by Germano *et al.* (1991) and the DMM, which is a linear combination of the SSM by Liu *et al.* (1994) and the DSM. The unresolved SFS stresses are modeled by the DSM, while the resolved SFS stresses are modeled by the SSM. Another aim of this work was to investigate whether the SSM by Liu *et al.* (1994) is an appropriate model for the resolved SFS stresses. The LES results predicted by the dynamic models using two- or three-dimensional test filtering are compared. The sharp cut-off filter is applied only in the two-dimensional test filtering, while the fourth-order commutative filter is applied using both two-dimensional and three-dimensional test filtering.

For two-dimensional test filtering, the DMM performs very well. The mean velocity profile predicted by the DMM is very similar to the profile by the DSM with the sharp cut-off filter. The DSM with the cut-off filter is known to produce good results in turbulent channel flows (Germano *et al.*, 1991; Piomelli *et al.*, 1988). Furthermore, a large improvement is observed for the turbulence intensities when using the DMM. The DSM with the commutative test filtering predicts results that deviate from the DNS data.

When using three-dimensional test filtering, the DMM also performs well as long as the grid resolution in the wall-normal direction is fine enough. The DMM requires a finer resolution in the wall-normal direction than the DSM to capture the log-law region of the mean velocity profile. It is the three-dimensional test filtering of the SSM portion that destroys the log-region. Even though the mean velocity profile is not correctly captured in the DMM results, the peak values of the turbulence intensities (in the near wall region) are well captured. The DSM again predicts results that differ to the DNS results when used with the three-dimensional commutative filter function. However, using a three-dimensional commutative test filter with the DSM, improves the mean velocity profiles when compared to the two-dimensional case. The improvements are not observed in the turbulence intensities which show almost no difference between two- or three-dimensional filtering.

The large deviation between the DNS data and the DSM results when using the fourth-order commutative filter function shows the need to use an SFS model for the resolved SFS stresses. The same trend is observed for both two- and three-dimensional test filtering. The increased value of the model coefficient in the DSM caused by using the smooth commutative test filter seems to be the reason for the increased disagreement between the LES results and the DNS data. The value of the model coefficient increases when used with the commutative test filter and this results in an increased eddy viscosity. The larger eddy viscosity enhances the over-prediction of both mean velocity profile and turbulence intensities.

The simulations using the DMM indicate that the SSM by Liu *et al.* (1994) is a very promising model for the resolved SFS stresses. The requirement for the

DMM to predict reasonable results is that the grid resolution is fine enough in the inhomogeneous direction. The concept of using a model parameter in the expression of the SSM needs to be investigated, but is left for future investigations.

The dynamic model coefficient is usually averaged in the homogeneous directions (Germano *et al.*, 1991), but since this averaging procedure is not always feasible, there is great interest to investigate how local averaging of the model coefficient affects the LES results. In this study, the local averaging was performed by filtering the coefficient using the commutative test filter function. The study is limited to the influence of the averaging procedure on the LES results predicted by the DSM when used with the fourth-order commutative test filter.

The simulations show that local averaging of the dynamic model coefficient improves the predicted LES results. The local averaging allows the coefficient to vary in the homogeneous directions, and it has a favorable impact on the predicted LES results. It is interesting to note that the use of a simple procedure such as local averaging has a significant impact on the results. Most likely, allowing the model coefficient to vary in the plane aids the break-up of large structures that are predicted in the near wall region. This allows the log-law region in the predicted mean velocity profile to approach the wall, thereby improving the results. The influence of local averaging with the DMM is also of interest, but is left for future studies.

In summary, the DMM performs best with the fourth-order commutative test filter function while the DSM with the same test filter shows the worst performance. Three-dimensional test filtering improves the results when compared to two-dimensional filtering. Using a smooth filter function with the DSM in implicitly filtered LES definitely shows the need for an SFS model for the resolved SFS stresses. The SSM by Liu *et al.* (1994) used as a model for the resolved SFS stresses gives reasonably good results as long as the grid resolution is fine enough in the inhomogeneous direction. Local averaging of the model coefficient in the DSM improves the predicted LES results when a smooth test filter function is used. This simple local averaging method seems to provide a promising alternative to more involved local models.

References

Bardina, J., Ferziger, J.H. and Reynolds, W.C. (1980), "Improved subgrid scale models for large eddy simulation", AIAA-80-1357.

Carati, D. and Eijnden, E.V. (1997), "On the self-similarity assumption in dynamic models for large eddy simulations", *Physics of Fluids*, Vol. 9, pp. 2165-7.

Carati, D., Winckelmans, G.S. and Jeanmart, H. (2001), "On the modelling of the subgrid-scale and filtered-scale stress tensors in large-eddy simulation", *Journal of Fluid Mechanics*, Vol. 441, pp. 119-38.

Chow, F.K. and Street, R.L. (2002), "Modeling unresolved motions in LES of field-scale flows", *American Meteorological Society, 15th Symposium on Boundary Layers and Turbulence*, pp. 432-5.

Dukowicz, J.K. and Dvinsky, A. (1992), "Approximation as a higher order splitting for the implicit incompressible flow equations", *Journal of Computational Physics*, Vol. 102, pp. 336-47.

Germano, M., Piomelli, U., Moin, P. and Cabot, W.H. (1991), "A dynamic subgrid-scale eddy viscosity model", *Physics of Fluids A*, Vol. 3, pp. 1760-5.

Ghosal, S. (1995), "An analysis of numerical errors in large-eddy simulations of turbulence", *Journal of Computational Physics*, Vol. 125, pp. 187-206.

Ghosal, S. and Moin, P. (1995), "The basic equations of the large eddy simulation of turbulent flows in complex geometry", *Journal of Computational Physics*, Vol. 118, pp. 24-37.

Ghosal, S., Lund, T.S., Moin, P. and Akselvoll, K. (1995), "A dynamic localization model for large-eddy simulation of turbulent flows", Vol. 286, pp. 229-55.

Gullbrand, J. (2000), "An evaluation of a conservative fourth order DNS code in turbulent channel flow", *Annual Research Briefs 2000*, Center for Turbulence Research, pp. 211-18.

Gullbrand, J. (2002), "Grid-independent large-eddy simulation in turbulent channel flow using three-dimensional explicit filtering", *Annual Research Briefs 2002*, Center for Turbulence Research, pp. 167-79.

Gullbrand, J. and Chow, F.K. (2003), "The effect of numerical errors and turbulence models in LES of channel flow, with and without explicit filtering", *Journal of Fluid Mechanics* (in press).

Lilly, D.K. (1992), "A proposed modification of the Germano subgrid-scale closure method", *Physics of Fluids A*, Vol. 4, pp. 633-5.

Liu, S., Meneveau, C. and Katz, J. (1994), "On the properties of similarity subgrid-scale models as deduced from measurements in a turbulent jet", *Journal of Fluid Mechanics*, Vol. 275, pp. 83-119.

Lund, T.S. (1997), "On the use of discrete filters for large eddy simulation", *Annual Research Briefs 1997*, Center for Turbulence Research, pp. 83-95.

Lund, T.S. and Kaltenbach, H-J. (1995), "Experiments with explicit filtering for LES using a finite-difference method", *Annual Research Briefs 1995*, Center for Turbulence Research, pp. 91-105.

Morinishi, Y., Lund, T.S., Vasilyev, O.V. and Moin, P. (1998), "Fully conservative higher order finite difference schemes for incompressible flow", *Journal of Computational Physics*, Vol. 143, pp. 90-124.

Moser, R.D., Kim, J. and Mansour, N.N. (1999), "Direct numerical simulation of turbulent channel flow up to $Re_\tau = 590$", *Physics of Fluids*, Vol. 11, pp. 943-5.

Najjar, F.M. and Tafti, D.K. (1996), "Study of discrete test filters and finite difference approximations for the dynamic subgrid-scale stress model", *Physics of Fluids*, Vol. 8, pp. 1076-88.

Piomelli, U., Moin, P. and Ferziger, J.H. (1988), "Model consistency in large eddy simulation of turbulent channel flows", *Physics of Fluids*, Vol. 31, pp. 1884-91.

Sarghini, F., Piomelli, U. and Balaras, E. (1999), "Scale-similar models for large-eddy simulations", *Physics of Fluids*, Vol. 11, pp. 1596-607.

Spalart, P., Moser, R. and Rogers, M. (1991), "Spectral methods for the Navier-Stokes equations with one infinite and two periodic directions", *Journal of Computational Physics*, Vol. 96, pp. 297-324.

Stolz, S., Adams, N.A. and Kleiser, L. (2001), "An approximate deconvolution model for large-eddy simulation with application to incompressible wall-bounded flows", *Physics of Fluids*, Vol. 13, pp. 997-1015.

Vasilyev, O.V. (2000), "High order finite difference schemes on non-uniform meshes with good conservation properties", *Journal of Computational Physics*, Vol. 157, pp. 746-61.

Vasilyev, O.V., Lund, T.S. and Moin, P. (1998), "A general class of commutative filters for LES in complex geometries", *Journal of Computational Physics*, Vol. 146, pp. 82-104.

Winckelmans, G.S., Jeanmart, H. and Carati, D. (2002), "On the comparison of turbulence intensities from large-eddy simulation with those from experiments or direct numerical simulation", *Physics of Fluids*, Vol. 14, pp. 1809-11.

Winckelmans, G.S., Wray, A.A., Vasilyev, O.V. and Jeanmart, H. (2001), "Explicit filtering large-eddy simulation using the tensor-diffusivity model supplemented by a dynamic smagorinsky term", *Physics of Fluids*, Vol. 13, pp. 1385-403.

Zang, Y., Street, R.L. and Koseff, J.R. (1993), "A dynamic mixed subgrid-scale model and its application to turbulent recirculating flows", *Physics of Fluids*, Vol. 5, pp. 3186-96.